JOINT POWER CONTROL AND SIGNATURE DESIGN FOR TIME-REVERSAL UPLINKS

Qinyi Xu, Yan Chen, and K. J. Ray Liu

University of Maryland College Park
Department of Electrical and Computer Engineering
College Park, MD, 20740, USA

ABSTRACT

In the time reversal division multiple access (TRDMA) system, the signal-to-noise ratio (SNR) is boosted and the inter-user interference (IUI) is suppressed due to the temporal and spatial focusing effects of the time-reversal (TR) technique. However, since the focusing effects highly depend on the location-specific multipath profile, there exists a strong-weak focusing effect in the TRDMA uplink system where different users at different locations enjoy different level of focusing effects. In this paper, we formulate the strong-weak focusing effect in the multiuser TRDMA uplink system as a max-min signal-to-interference-noise ratio (SINR) balancing problem by means of joint power control and signature filter design. A novel two-stage adaptive algorithm that can guarantee the convergence is proposed. Numerical results show that our algorithm converges quickly, achieves a high energy-efficiency gain, and provides a performance guarantee to all users.

Index Terms— Time reversal, strong-weak focusing effect, energy efficiency, QoS guarantee.

1. INTRODUCTION

The explosive growth of high speed wireless services that can support various wireless communication applications with a large number of users calls for future wideband communication solutions. The dispersion of a channel in wideband communications will bring in an undesirable phenomenon: inter-symbol interference (ISI).

Thanks to its inherent nature that fully collects energy of multi-path propagation, the time-reversal (TR) based signal transmission is an ideal paradigm for low-complexity single-carrier broadband communication systems [1–4]. In essence, by treating each path of the multi-path channel in a rich scattering environment as a widely distributed virtual antenna, TR provides a high-resolution spatial focusing effect so that it can alleviate inter-user interference (IUI) effectively. Meanwhile, the traditional TR signature works as a matched filter at the access point (AP), which brings a temporal focusing effect that boosts the signal-to-noise ratio (SNR).

The temporal and spatial focusing effects of the TR have been proposed as theory and validated through experiments in both acoustic domain and radio frequency (RF) domain. As verified in [5–12], energy of acoustic signal can be refocused with high resolution through a time-reversal mirror (TRM), a self-adaptive technique that can be utilized to compensate for propagation distortions. The theory of TRM is formally developed for electromagnetic waves in [13]. However, since the quality of temporal and spatial focusing effects of EM waves highly depends on the propagation environment and transmission bandwidth, there exists a "strong-weak" effect in the multiuser TRDMA uplink system, where the received SNRs of different users can be very different and weak signals can be blocked from correct detection in the presence of strong ones. Fig. 1 illustrates the detectability problem for TRDMA uplink system where K users transmit simultaneously and possess different focusing effects denoted by the amplitude of waves above different paths.

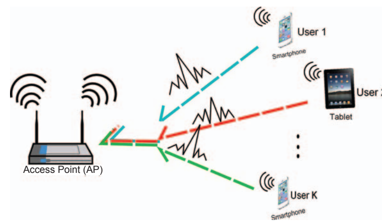

Fig. 1. Representative case for TRDMA uplink system.

Unlike the CDMA near-far problem resulted solely from distance [14], the TRDMA uplink systems suffer from the strong-weak focusing effect among different users mainly due to the different resonances resulted from location-specific multipath environments. To guarantee the performance, we need to combat the strong-weak focusing effect and balance the signal-to-interference-noise ratios (SINRs) among all links. To this end, we formulate the strong-weak focusing effect combating problem in the TRDMA uplink system as a max-min SINR optimization problem by the means of joint power allocation and signature filter design. In this work, we propose a two-stage algorithm that solves this problem efficiently and converges to the global optimum quickly. Simulation results demonstrate that the proposed algorithm is capable of providing a performance guarantee to all users

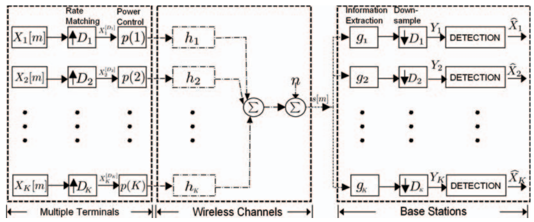

Fig. 2. Diagram for TRDMA uplink system.

regardless of their channel gains. Furthermore, our proposed algorithm is highly energy efficient comparing to the basic TR schemes [2].

This paper is organized as follows. In Section 2, the system model and problem formulation is described. In Section 3.1, we relax the original TRDMA uplink SINR balancing problem into an eigenvalue optimization problem. The two-stage adaptive algorithm for the TRDMA uplink SINR balancing problem with individual constraints is proposed in Section 3.2. Numerical simulation in Section 4 demonstrates the performance improvement and conclusion is drawn in Section 5.

2. SYSTEM MODEL

According to the system diagram in Fig. 2 [4], the received signal at the AP can be written as

$$\mathbf{s} = \sum_k \sqrt{p(k)}\mathbf{H}_k\mathbf{x}_k + \mathbf{n}, \tag{1}$$

where $\mathbf{s}$ is a $(2L-1)\times 1$ vector with $L = max_k\ L_k$, $\mathbf{H}_k$ is a $(2L-1)\times L$ Toeplitz matrix with each column being the shifted version of $\mathbf{h}_k$, and $\mathbf{n}$ denotes the additive white Gaussian noise (AWGN) vector whose elements are identical complex Gaussian with mean zero and variance σ^2.

At the AP side, the received signal $\mathbf{s}$ will be first passed through a user-specific signature filter bank $\{\mathbf{g}_i,\ \forall\ i\}$ to extract information and suppress interference, and then downsampled to obtain Y_i.

The system uplink SINR for user i is given as,

$$SINR_i^{UL}(\mathbf{G},\ \mathbf{p}) = \frac{p(i)\mathbf{g}_i^H\mathbf{R}_i^{(0)}\mathbf{g}_i}{p(i)\mathbf{g}_i^H\hat{\mathbf{R}}_i\mathbf{g}_i + \sum_{j\neq i}p(j)\mathbf{g}_i^H\mathbf{R}_j\mathbf{g}_i + \sigma^2}, \tag{2}$$

where $\mathbf{G} = [\mathbf{g}_1,\ \cdots,\ \mathbf{g}_K]$ is the signature matrix, $\mathbf{p} = [p(1),\ \cdots,\ p(K)]^T$ is the power allocation vector, $\mathbf{R}_i^{(0)} = \mathbf{H}_i^{(L)H}\mathbf{H}_i^{(L)}$ with $\mathbf{H}_i^{(l)}$ being the l^{th} row of $\mathbf{H}_i$, $\mathbf{R}_j = \tilde{\mathbf{H}}_j^H\tilde{\mathbf{H}}_j$, $\tilde{\mathbf{H}}_j$ is the upsampled version of $\mathbf{H}_j$ with factor D_j and sampling center located at $\mathbf{H}_j^{(L)}$, and $\hat{\mathbf{R}}_i = \mathbf{R}_i - \mathbf{R}_i^{(0)}$. $p(i)\mathbf{g}_i^H\hat{\mathbf{R}}_i\mathbf{g}_i$ and $\sum_{j\neq i}p(j)\mathbf{g}_i^H\mathbf{R}_j\mathbf{g}_i$, represent ISI and IUI respectively.

Let us define a crosstalk matrix $\mathbf{\Phi}$ for the TRDMA uplink system whose elements correspond to the ISI and IUI term in $SINR_i^{UL}$ as $[\mathbf{\Phi}]_{ij} = \mathbf{g}_j^H\mathbf{R}_i\mathbf{g}_j$, when $i \neq j$ and $[\mathbf{\Phi}]_{ij} = \mathbf{g}_i^H\hat{\mathbf{R}}_i\mathbf{g}_i$, if $i = j$. Moreover, $\mathbf{D}$ is defined as a diagonal matrix with $[\mathbf{D}]_{ii} = \gamma_i/\mathbf{g}_i^H\mathbf{R}_i^{(0)}\mathbf{g}_i$, and γ_i is the weighted factor for i^{th} user. In order to ensure the fairness for all users and boost the system performance, we jointly design the signature matrix $\mathbf{G}$ and power allocation vector $\mathbf{p}$ by balancing the $SINR_i^{UL}(\mathbf{G},\ \mathbf{p})$ among different users, i.e., the max-min fairness is adopted in this work as follows

$$\begin{aligned} \underset{\mathbf{G},\ \mathbf{p}}{\text{maximize}}\ \ & \min_j \frac{p(j)}{[\mathbf{D}]_{jj}(\mathbf{\Phi}_j^T\mathbf{p}+\sigma^2)} \\ \text{subject to}\ \ & \mathbf{p}\succeq\mathbf{0},\ \mathbf{p}\preceq\mathbf{p}_{max}, \|\mathbf{g}_i\|_2 = 1, \forall i. \end{aligned} \tag{3}$$

where $\mathbf{p}_{max}$ is the maximal value of transmitting power for each individual users, and $\mathbf{0}$ is an all-zero vector.

3. TWO-STAGE ADAPTIVE ALGORITHM FOR INDIVIDUAL SINR BALANCING

3.1. Relaxed Total Power Constraint Problem

In this section, we will introduce our work on relaxing the original uplink SINR balancing problem into an equivalent eigenvalue optimization problem and introduce the proposed algorithm where the signature and power assignment are iteratively optimized.

The relaxed version of the original problem in (3) is

$$\begin{aligned} \underset{\mathbf{G},\ \mathbf{p},\ \gamma}{\text{maximize}}\ \ & \gamma \\ \text{subject to}\ \ & \mathbf{p}\succeq\mathbf{0},\ \mathbf{p}\succeq\gamma\mathbf{D}(\mathbf{\Phi}^T\mathbf{p}+\boldsymbol{\sigma}), \\ & \mathbf{1}^T\mathbf{p}\leq\mathbf{1}^T\mathbf{p}_{max},\ \|\mathbf{g}_i\|_2 = 1, \forall i, \end{aligned} \tag{4}$$

where $\mathbf{1}$ is an all-one vector with K elements.

We first consider the case when the signature matrix is fixed as $\tilde{\mathbf{G}}$, and then problem in (4) is reduced to an uplink power allocation problem as

$$\begin{aligned} \underset{\mathbf{p},\ \gamma}{\text{maximize}}\ \ & \gamma \\ \text{subject to}\ \ & \mathbf{p}\succeq\mathbf{0},\ \mathbf{p}\succeq\gamma\mathbf{D}(\mathbf{\Phi}^T\mathbf{p}+\boldsymbol{\sigma}) \\ & \mathbf{1}^T\mathbf{p}\leq\mathbf{1}^T\mathbf{p}_{max}. \end{aligned} \tag{5}$$

Theorem 1 *Given $\tilde{\mathbf{G}}$, the necessary condition for the global optimum $\boldsymbol{p}^*$ can be characterized as an eigensystem that*

$$\frac{1}{\gamma^*}\tilde{\boldsymbol{p}}^* = \Lambda(\boldsymbol{G}, P_{total})\tilde{\boldsymbol{p}}^*, \tag{6}$$

where γ^* is the optimum of weighted SINR threshold, $\tilde{\boldsymbol{p}} = [\boldsymbol{p}^T,\ 1]^T$, $P_{total} = \boldsymbol{1}^T\boldsymbol{p}_{max}$ and $\boldsymbol{\Lambda}(\boldsymbol{G}, P_{total})$ is an augmented matrix as

$$\boldsymbol{\Lambda}(\boldsymbol{G}, P_{total}) = \begin{pmatrix} \boldsymbol{D\Phi^T} & \boldsymbol{D\sigma} \\ \frac{1}{P_{total}}\boldsymbol{1}^T\boldsymbol{D\Phi^T} & \frac{1}{P_{total}}\boldsymbol{1}^T\boldsymbol{D\sigma} \end{pmatrix}. \tag{7}$$

In TRDMA uplink systems, $\mathbf{\Lambda}(\mathbf{G}, P_{total})$ is a matrix with nonnegative entry and is also irreducible. According to the Perron Frobenius Theorem [15–17], there exists a feasible solution to (6) and the solution is unique. The necessary condition in 6 is actually a necessary and sufficient condition for global optimum. Thus, the power allocation problem in

Algorithm 1 Iterative SINR Balancing Algorithm under Total Power Constraint

Initialize for $n = 0$.
loop Calculate $\mathbf{g}_i^{(n)},\ \forall\ i$ using MMSE method with $\mathbf{p}^{(n-1)}$ and $\|\mathbf{g}_i\|_2 = 1,\ \forall\ i$.
  Build the couple matrix $\mathbf{\Lambda}^{(n)}(\mathbf{G}^{(n)}, P_{total})$.
  Solve the Perron Frobenius eigenpair problem in (6) and get $\lambda_{max}^{(n)}$ and its corresponding eigenvector $\tilde{\mathbf{p}}^{(n)}$ with $\tilde{p}^{(n)}(K+1) = 1$. $\mathbf{p}^{(n)} \leftarrow \{\tilde{\mathbf{p}}^{(n)}\}_1^K$.
end loop If $\lambda_{max}^{(n-1)} - \lambda_{max}^{(n)} < \epsilon$ or reach the maximal number of iterations.

(5) is equivalent to find the Perron Frobenius eigenvector of $\mathbf{\Lambda}(\tilde{\mathbf{G}}, P_{total})$.

Based upon the previous analysis, the (4) is equivalent to an eigenvalue optimization problem as

$$\begin{aligned} &\underset{\mathbf{G}}{\text{minimize}}\ \ \lambda_{max}(\mathbf{\Lambda}(\mathbf{G}, P_{total})) \\ &\text{subject to}\ \ \|\mathbf{g}_i\|_2 = 1,\ i = 1, \ldots, K, \end{aligned} \tag{8}$$

Let us define a cost function as

$$\tilde{\lambda}(\mathbf{G}, \mathbf{p}) \ = \ \max_{\mathbf{x} \succ 0} \frac{\mathbf{x}^T \mathbf{\Lambda}(\mathbf{G}, P_{total}) \tilde{\mathbf{p}}}{\mathbf{x}^T \tilde{\mathbf{p}}}, \tag{9}$$

and the Perron Frobenius eigenvalue can be represented as $\lambda_{max}(\mathbf{\Lambda}(\mathbf{G}, P_{total})) = \min_{\mathbf{p} \succ 0} \tilde{\lambda}(\mathbf{G}, \mathbf{p})$.

Lemma 1 *The optimal signature matrix for a given vector* $\boldsymbol{p}_{ary}$ *is denoted as* $\boldsymbol{G}^*$. *Then, we have*

$$\boldsymbol{G}^* = arg \min_{\boldsymbol{G}} \tilde{\lambda}(\boldsymbol{G}, \boldsymbol{p}_{ary}) \tag{10}$$

That is to say, the optimal signature can be obtained by individually maximizing the uplink SINR of each user.

Remark: The solution is equivalent to the MMSE beamforming, $\mathbf{g}_i^* \ = \ \alpha_i(\sum_{j=1}^K p_{ary}(j)\mathbf{R}_j \ + \ \sigma^2 \mathbf{I})^{-1}\mathbf{H}_i^{(L)H}, \forall i$, where α_i is a normalized vector.

The necessary and sufficient condition for the global optimum of problem in (8) is stated in Theorem 2.

Theorem 2 (*Necessary and Sufficient Condition*) $\boldsymbol{G}^* = [\boldsymbol{g}_1^*,\ \boldsymbol{g}_2^*,\ \cdots,\ \boldsymbol{g}_K^*]$ *is the global optimizer of the problem in (8) if and only if* $\tilde{\lambda}(\boldsymbol{G}^*, \boldsymbol{p}^*) = \min_{\boldsymbol{G}} \tilde{\lambda}(\boldsymbol{G}, \boldsymbol{p}^*)$, *where* $\boldsymbol{p}^* = arg \min_{\boldsymbol{p} \succ \boldsymbol{0}} \tilde{\lambda}(\boldsymbol{G}^*, \boldsymbol{p})$, *i.e.,* $\tilde{\boldsymbol{p}}^*$ *is the solution to the Perron Frobenius eigenvalue problem of* $\mathbf{\Lambda}(\boldsymbol{G}^*, P_{total})$.

Theorem 2 implies that if one of the variable $\mathbf{p}$ or $\mathbf{G}$ has reached the global optimum, the remaining one can be obtained by either solving the Perron Frobenius eigenpair problem in (6) or by independently solving the MMSE problem. Based on this, we propose Algorithm 1 that alternatively optimizes $\mathbf{p}$ and $\mathbf{G}$, and eventually converges to the global optimum.

The necessary and sufficient condition for global optimum is equivalent to the condition $\lambda_{max}^{(n+1)} = \lambda_{max}^{(n)}$. As a consequence, the algorithm can be stopped as soon as the difference in $\lambda_{max}^{(n-1)} - \lambda_{max}^{(n)}$ reaches a predetermined threshold $\epsilon > 0$. On average the algorithm will yield the global optimum in 3 or 4 iterations.

Algorithm 2 Two-Stage Adaptive Algorithm for SINR Balancing Problem under Individual Power Constraint

Initialize $\mathbf{p}^{(0)}$ with $P_{total}^{(0)} = \mathbf{1}^T \mathbf{P}_{max}$, $\delta \mathbf{p}^{(0)} \leftarrow \mathbf{P}_{max} - \mathbf{p}^{(0)}$, [index, $\delta^{(0)}$] $\leftarrow$ min($\delta \mathbf{p}^{(0)}$)
loop $\mathbf{p} \leftarrow$ by Algorithm 1 with $0.9P_{total}^{(n-1)}$,
  Approximated gradient slope $\leftarrow \frac{\mathbf{p}^{(n-1)}(\text{index}) - \mathbf{p}(\text{index})}{0.1P_{total}}$.
  $\delta P_{total} \leftarrow \frac{\delta^{(n-1)}}{\text{slope}}$, $P_{total}^{(n)} \leftarrow P_{total}^{(n-1)} + \delta P_{total}$.
  Update $\mathbf{p}^{(n)}$ and $\delta \mathbf{p}^{(n)}$, [index, $\delta^{(n)}$] $\leftarrow$ min($\delta \mathbf{p}^{(n)}$)
  while $\delta^{(n)} > \epsilon$ **do**
    $\delta P_{total} \leftarrow \eta \delta P_{total}$. Update $P_{total}^{(n)}$, $\mathbf{p}^{(n)}$, and $\delta^{(n)}$
  end while
end loop If $|\delta^{(n)}| \leq \epsilon$ or reach the maximal number of iterations.

3.2. Two-stage Solution for Individual Constraints

From the previous section, for any fixed total power constraint value P_{total}, there only exists one pair of optimal signature matrix $\mathbf{G}^*(P_{total})$ and power assignment vector $\mathbf{p}^*(P_{total})$. However, the original problem with individual power constraints has a more tightened feasible set.

Lemma 2 *The optimal power assignment vector generated from iterative SINR balancing algorithm in Algorithm 1 is monotonically increasing as the total power constraint* P_{total} *increases.*

According to Lemma 2, we know that as the feasible set is shrunk by reducing the total power constraint in (4), the optimal power assignment for each user is monotonically decreasing. As long as we keep adjusting the feasible set bounded by the total power constraint, we will definitely reach a point where the optimal power assignment for at least one user is equal to his constraint and the others are below the constraints. At this point, we achieve the maximum of feasible threshold.

The proposed two-stage adaptive algorithm is shown in Algorithm 2, where the SINR balancing problem with individual constraints is solved in two alternative and iterative stages. In stage I, the corresponding global optimum of the relaxed eigenvalue optimization problem is obtained via Algorithm 1. In stage II, the relaxed feasible set is modified by updating the total power constraint using the gradient decent method against the worst case. On average 3 iterations are needed for Algorithm 2 to find the optimal solution.

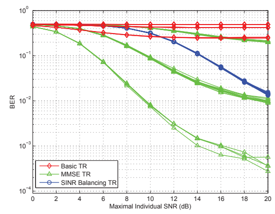

Fig. 3. BER Performance.

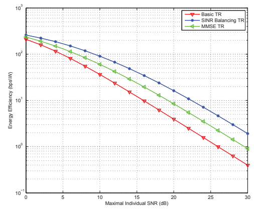

Fig. 4. Energy Efficiency.

4. SIMULATION RESULTS

To evaluate the proposed algorithms, we conduct several simulations to demonstrate that our proposed SINR balancing algorithm is an ideal solution to ensure fairness and energy-efficiency and to tackle the strong-weak effects. The simulation settings are: 1. Channel Model: UWB office non-line-of-sight channel with $B = 500\ MHz$ and $L = 60$; 2. equal weighted factor γ_i and equal maximal power constraint.

4.1. Highly Crowded Network

In this part, we simulate a highly crowded network where one AP serves 20 users. We assume the 20 users are divided into 3 groups according to their channel gains. In MMSE TR, each user also transmits in the maximal power but its signature $\mathbf{g}$ is the MMSE signature that can be calculated by independently maximizes its own SINR. In Basic TR scheme, each user transmits with its maximal power and the signature filter $\mathbf{g}_i$ is,

$$g_i[k] = \frac{h_i^*[L-1-k]}{\sqrt{\sum_{l=0}^{L-1}|h_i[l]|^2}}, \quad k = 0,\ 1,\ 2,\ \cdots,\ L-1. \quad (11)$$

In Fig. 3, we can see the BER performances of the aforementioned three schemes in a highly crowded network and the proposed SINR balancing scheme is capable to provide a service guarantee for all users. With the objective to balance the uplink SINR at the receiver side, our scheme achieves the same BER performance for all users, which is much better than the worst BER case in other two schemes. In basic TR, the whole system fails to work properly due to high BERs. With MMSE TR, some of users whose channel degradation is severe will have a poor BER performance that is close to the basic TR BER curves and get blocked out. These blocked users bring high interference to other active users which degrades the whole network's performance. When applying our proposed algorithm to this crowded network, as SINRs are balanced, all users will have almost the same BER performance such that all of them can be detected.

The energy-efficiency feature of our proposed scenario is further studied in Fig. 4. Here, we define the energy efficiency as the ratio between achievable sum rate and the total transmitted power of all users, i.e. Energy Efficiency $= \frac{\text{Achievable Sum Rate (bps)}}{\text{Total Power Consumed (W)}}$. Fig. 4 illustrates that the system energy efficiency can be improved remarkably. The reason is that through power control the interference between users can be managed and the signature matrix at the receiver side further alleviates the IUI and ISI leading to a transmit power reduction. Thus the whole system can utilize the entire resource more efficiently.

4.2. Comparison under Different Backoff Rates

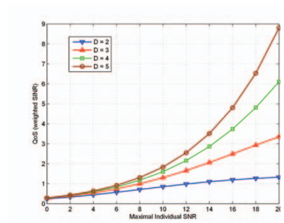

Fig. 5. Balanced SINR.

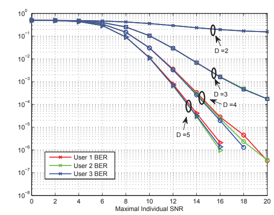

Fig. 6. BER Performance.

In Fig. 5 and 6, the performance of our proposed algorithm under different backoff rates is studied. For a smaller D, the uplink transmission is conducted more frequently which causes the ISI to lie close to the signal peak at the receiver side. On the contrary, IUI and ISI can be significantly alleviated by choosing a higher backoff rate D. In Fig. 5, the balanced SINR becomes higher as the backoff rate increases. As BER is a monotonically decreasing function in uplink SINR, users' BER in our scheme is also reducing as the backoff rate increases as shown in Fig. 6. However, because the achievable sum rate is normalized by $1/D$, a higher D may result in a smaller sum rate.

5. CONCLUSION

In this paper, we propose a joint power allocation and signature design method to address the strong-weak focusing effect in time-reservation uplink systems. By forming the strong-weak focusing effect problem into a max-min SINR problem, a two-stage adaptive algorithm is proposed. In stage I, the original non-convex optimization problem is relaxed into a Perron Frobenius eigenvalue optimization problem whose optimum can be efficiently obtained. In stage II, the gradient descent method is applied to iteratively update the feasible set until all individual constraints are satisfied. The proposed algorithm converges in a few iterations with a relatively low computational complexity. Simulation results show that the proposed algorithm provides a high energy-efficiency gain and a performance guarantee to all users in network and thus it is a promising technique for energy-efficient QoS-guaranteed TRDMA uplink systems.

References

[1] Beibei Wang, Yongle Wu, Feng Han, Yuhan Yang, and K. J. Ray Liu, "Green wireless communications: A time-reversal paradigm," *Selected Areas in Communications, IEEE Journal on*, vol. 29, no. 8, pp. 1698–1710, September 2011.

[2] Feng Han, Yuhan Yang, Beibei Wang, Yongle Wu, and K. J. Ray Liu, "Time-reversal division multiple access over multi-path channels," *Communications, IEEE Transactions on*, vol. 60, no. 7, pp. 1953–1965, July 2012.

[3] Yan Chen, Yuhan Yang, Feng Han, and K. J. Ray Liu, "Time-reversal wideband communications," *Signal Processing Letters, IEEE*, vol. 20, no. 12, pp. 1219–1222, Dec 2013.

[4] Yan Chen, Feng Han, Yu-Han Yang, Hang Ma, Yi Han, Chunxiao Jiang, Hung-Quoc Lai, D. Claffey, Z. Safar, and K. J. Ray Liu, "Time-reversal wireless paradigm for green internet of things: An overview," *Internet of Things Journal, IEEE*, vol. 1, no. 1, pp. 81–98, Feb 2014.

[5] M. Fink, C. Prada, F. Wu, and D. Cassereau, "Self focusing in inhomogeneous media with time reversal acoustic mirrors," in *Ultrasonics Symposium, 1989. Proceedings., IEEE 1989*, Oct 1989, pp. 681–686 vol.2.

[6] M. Fink, "Time reversal of ultrasonic fields. i. basic principles," *Ultrasonics, Ferroelectrics, and Frequency Control, IEEE Transactions on*, vol. 39, no. 5, pp. 555–566, Sept 1992.

[7] F. Wu, Jean-Louis Thomas, and M. Fink, "Time reversal of ultrasonic fields. il. experimental results," *Ultrasonics, Ferroelectrics, and Frequency Control, IEEE Transactions on*, vol. 39, no. 5, pp. 567–578, Sept 1992.

[8] WA Kuperman, William S Hodgkiss, Hee Chun Song, T Akal, C Ferla, and Darrell R Jackson, "Phase conjugation in the ocean: Experimental demonstration of an acoustic time-reversal mirror," *The journal of the Acoustical Society of America*, vol. 103, no. 1, pp. 25–40, 1998.

[9] Hee Chun Song, WA Kuperman, WS Hodgkiss, T Akal, and C Ferla, "Iterative time reversal in the ocean," *The Journal of the Acoustical Society of America*, vol. 105, no. 6, pp. 3176–3184, 1999.

[10] Daniel Rouseff, Darrell R Jackson, Warren LJ Fox, Christopher D Jones, James A Ritcey, and David R Dowling, "Underwater acoustic communication by passive-phase conjugation: Theory and experimental results," *Oceanic Engineering, IEEE Journal of*, vol. 26, no. 4, pp. 821–831, 2001.

[11] G Lerosey, J De Rosny, A Tourin, A Derode, G Montaldo, and M Fink, "Time reversal of electromagnetic waves and telecommunication," *Radio science*, vol. 40, no. 6, 2005.

[12] G Lerosey, J De Rosny, A Tourin, A Derode, and M Fink, "Time reversal of wideband microwaves," *Applied Physics Letters*, vol. 88, no. 15, pp. 154101–154101, 2006.

[13] Julien de Rosny, Geoffroy Lerosey, and Mathias Fink, "Theory of electromagnetic time-reversal mirrors," *Antennas and Propagation, IEEE Transactions on*, vol. 58, no. 10, pp. 3139–3149, 2010.

[14] Theodore S. Rappaport, *Wireless Communications: Principles and Practice*, IEEE Press, Piscataway, NJ, USA, 1st edition, 1996.

[15] E. Seneta, *Non-negative Matrices and Markov Chains*, Springer series in statistics. Springer, 2006.

[16] A.V. Arkhangel'skiĭ and L.S. Pontryagin, *General Topology I Basic Concepts and Constructions Dimension Theory*, Number v. 1-3 in Encyclopaedia of mathematical sciences. Springer-Verlag, 1990.

[17] Weidong Yang and Guanghan Xu, "Optimal downlink power assignment for smart antenna systems," in *Acoustics, Speech and Signal Processing, 1998. Proceedings of the 1998 IEEE International Conference on*, May 1998, vol. 6, pp. 3337–3340 vol.6.